Continuous-Phase Mass-Transfer Coefficients for Liquid Extraction in Agitated Vessels

HARVEY D. SCHINDLER and ROBERT E. TREYBAL

New York University, New York, New York

Area-free continuous-phase mass-transfer coefficients for continuous flow of ethyl acetate (dispersed) and water (continuous) were measured in a 9.5 in. diameter baffled vessel, agitated with 3 and 5 in. diameter flat-blade turbines, and with the 3 in. turbine in the absence of baffles. Specific interfacial area was determined by a light-transmission technique which permitted a vertical traverse of the vessel.

The specific area is greatest, and mean drop diameter smallest, near the impeller. The mean area is lower than that predicted from existing correlations for batch operation in the absence of mass transfer. Continuous-phase mass-transfer coefficients increase with increased impeller Reynolds number and dispersed-phase holdup, and are about 2.5 times larger in the unbaffled vessel at the same impeller power. The coefficients are generally larger than those predicted by existing correlations based on suspended solids, and it is suggested that this and the effect of holdup is the result of drop coalescence and redispersion, which causes a renewal of the continuous phase surrounding each drop. Rough estimates of the minimum coalescence frequency in the baffled vessel and application of the renewal concept to the data appear to confirm this view. Lack of information on circulation rates prevents immediate test of the data from the unbaffled vessel.

Mechanically stirred vessels are used extensively for liquid extraction in mixer-settler stages and incorporated directly or with modifications in most of the multistage tower extractors which have become popular in recent years (*1, 27*). This paper reports what are believed to be the first area-free mass-transfer coefficients for the continuous phase in continuously operated vessels, together with subsidiary data of interest, and a suggestion regarding the importance of drop coalescence and break-up to the phenomena observed.

Most of the available reports on the extraction characteristics of these vessels provide only scattered and uncorrelated data on stage efficiency, or, what is equivalent, the product Ka_{av}, where K combines the individual mass-transfer coefficients of the continuous (k_C) and dispersed (k_D) phases, and a_{av} is the specific interfacial area (*36*). The individual coefficients included in K can be expected to depend quite differently on conditions (impeller speed, vessel geometry, liquid properties, etc.) and it will therefore be ultimately necessary to know them separately. Nagata (*24*) measured $k_C\ a_{av}$ by dissolving O-toluidine drops dispersed in water, and determined a_{av} from drop sizes in samples withdrawn from the vessel. That work was done with very dilute dispersions ($\phi_D = 0.0063$) and there is uncertainty as to whether the drops did not coalesce during withdrawal. By choosing a transferring solute with a low solubility in the continuous phase, Rushton, et al. (*31*) measured Ka_{av} nearly equal to $k_C\ a_{AV}$ at $\phi_D = 0.082$. The results at this holdup are different from Nagata's. In any event, both of these studies were for batches of liquid, and the applicability to continuous flow is unknown. Reviews of work on k_C for solids suspended in liquids (*22, 23*) and of interfacial area of batch liquid dispersions (*36*) show the coefficient and area to be differently dependent upon operating conditions, although of course the applicability of these k_C's to liquids and of the batch areas to continuous flow is uncertain.

In the present work, interfacial area was determined *in situ* by a light-transmission technique adapted from the work of Rodger (*28* to *30*). Mass-transfer coefficients for the continuous phase alone were determined by contacting a dispersed phase of water-saturated ethyl acetate with a continuous phase of water. This technique (*9*) contains several built-in limitations. The mutual solubility of the contacted liquids must be sufficiently great so that adequate change in composition of the continuous phase occurs to permit good measurement. Yet high solubility inevitably leads to low interfacial tension, very large interfacial area, and such rapid mass transfer that the liquids emerge from the vessel essentially mutually saturated and coefficients become impossible to measure. The chosen liquid pair is satisfactory, but there are very few others. The remarkably high stage efficiency of a well-agitated vessel strongly limits the conditions studied to relatively low agitation intensities and low dispersed-phase holdup to keep the interfacial area small, and high flow rates to reduce holding time, all to prevent near equilibrium of the effluents. The high flow rates make experimentation very expensive.

EQUIPMENT AND PROCEDURES

The mixing vessel, Figure 1, was a glass cylinder, 9.5 in. I.D. by 9.5 in. tall, closed by stainless steel plates. For most of the work, four equally spaced, radial, vertical wall baffles, 0.95 in. wide, were installed. A circular glass window installed flush in the bottom plate permitted photographing the dispersion for purposes of calibrating the light-transmission apparatus. Openings at the top permitted introduction of sampling devices and a thermometer. A stainless steel, six flat-blade turbine impeller, dimensionally similar to those recommended by Rushton and Oldshue (*32*) was located at the center of the vessel. Two diameters, 3 and 5 in., were used in the baffled vessel, and one (3 in.) in the absence of baffles. Liquids were pumped through rotameters continuously into the center of the bottom, and the dispersion left at the top of the vessel, as shown.

The light-transmission apparatus included two ⅜ in. diam. Pyrex glass rods, platinized on the cylindrical surface, with ends square and polished. These were arranged on the same axis, passing through the upper and lower plates of the vessel

Harvey D. Schindler is presently with the Lummus Company, Bloomfield, New Jersey.

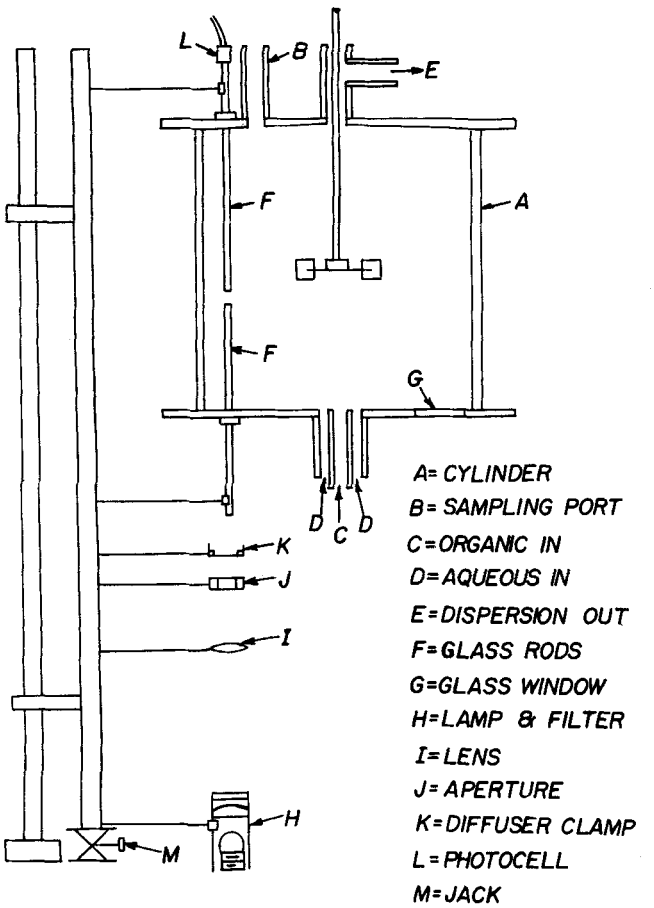

Fig. 1. Schematic diagram of apparatus.

at 3.2 in. from the vessel axis and midway between adjacent baffles. Light from a microscope lamp passed through the several focusing devices and filters shown in Figure 1, through the lower glass rod, a 1.75 cm. gap through which dispersion passed, the upper glass rod, and into a photoelectric cell. Current from the photocell was amplified by an electronic circuit essentially the same as that used by Rodger (29), modified so as to shorten the response time. The theory and application of such devices to the measurement of interfacial area has been fully described elsewhere (*28 to 30*). In this work, the entire light circuit of the device was securely mounted on an external rod to permit the gap between the glass rods to be moved vertically for the entire height of the vessel, so that a vertical profile of interfacial area for each run was obtained. Great care was taken to maintain constancy of gap width and truly axial location of the glass rods during such a traverse. This was checked by measurement of the gap with a cathetometer, and observing constancy of the photocell current when the gap was moved through the vessel filled only with water.

In order to calibrate the light transmission device, photographs were taken of the dispersion through the bottom glass window while the gap between the glass rods was located at the extreme bottom of the vessel. During these measurements the vessel was operated batch-like with mutually saturated liquids. Each photograph showed the image of a 0.0205 in. diam. hypodermic tube mounted on the upper side of the glass window to establish a length standard. The developed film was projected onto a screen and when the drop-size distribution was obtained, an interfacial area was computed and related to the photocell current. Photographs were also taken during each continuous flow run.

During continuous operation, measurements were begun after ten vessel volumes of liquid had passed through. Following the light-transmission traverse, samples of the continuous aqueous phase were taken at the top, center, and bottom of the vessel by withdrawal through a tubular, fritted-glass filter (medium porosity, average opening 15μ). This effectively filtered out the organic droplets. The filter was encased in a stainless steel tube, stoppered at the bottom, and arranged so that the filter was protected from contact with the liquids until it had been lowered to the desired position. The tube was removed during the actual sampling. Two samples of both phases for phase-ratio determinations were taken at the same locations by a thief made from a burette tube. After the thief was withdrawn, the sampled phases were equilibrated, their volumes measured, and analyzed. From their densities and concentrations, and those of the liquids in the vessel, the phase ratios as they existed in the vessel at the position of sampling were computed.

The ethyl acetate assayed 99.9 wt. %, refractive index of samples from various drums 1.37207 to 1.37248 at 20°C. (accepted value 1.37216 at 18.9°C.) It was saturated with water and used only once. The water was condensed steam, filtered as a liquid through a glass frit similar to that described above (refractive index 1.33300 ± 0.00010 at 20.0°C.). Interfacial tension between the saturated solutions was 6.40 dynes/cm. at 25.0°C. (accepted value 6.410). Every precaution was taken to keep the liquids thoroughly clean. When a drop of ester saturated with water was suspended from a capillary tube in water, no evidence of interfacial turbulence during dissolution of the drop could be observed. Aqueous solutions were analyzed with a Bausch and Lomb precision refractometer. This produced a maximum error of 0.037 wt. % ester, and on the average about a 5% error in the difference of concentrations of samples and the saturated water solution ($C_{A1} - C_{A2}$).

The operating conditions for mass-transfer studies were: total flow rate = 600 to 1,982 lb./hr.; feed ratio = 0.05 to 0.276 lb. organic/lb. water; impeller Reynolds number = 19,800 to 55,100. A great many other details are available elsewhere (*33*), including tables of data.

CONDITIONS AT THE BOTTOM OF THE VESSEL

Since many conclusions in respect to area and drop size derive from the data collected at the bottom of the vessel, it is important to outline what these data show.

Figure 2 is typical of the light-transmission calibration data. Here the specific area is computed from the mean drop size, d_p, observed in the photographs,

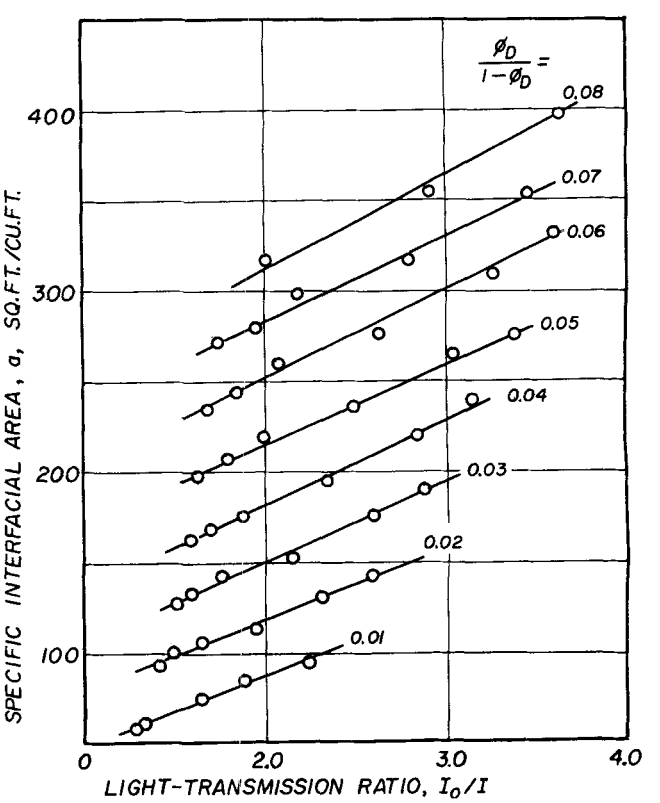

Fig. 2. Specific interfacial area calibration; 3 in. impeller, baffled vessel.

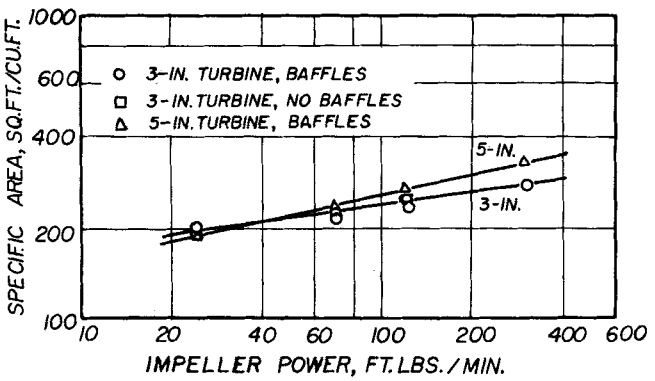

Fig. 3. Specific area at vessel bottom, $\phi_D = 0.02$.

$$d_p = \frac{\Sigma n_i d_i^3}{\Sigma n_i d_i^2} \quad (1)$$

and the relation

$$a = \frac{6\phi_D}{d_p} \quad (2)$$

Although derived from data at the bottom of the vessel under batch conditions, the calibrations are applicable to positions throughout the vessel and for continuous flow.

The specific area at the bottom is in general substantially smaller than that predicted from the correlations of Calderbank (5), Kafarov (20), and Vermeulen (38), whose work was reported for regions near the impeller tip and is therefore probably not really applicable. Thornton's correlation (35) is for a_{av} and gives results roughly in agreement with the observed areas, but indicates a more rapid increase with impeller speed than that observed. Figure 3 shows that the area produced in baffled and unbaffled vessels by the 3 in. impeller is the same

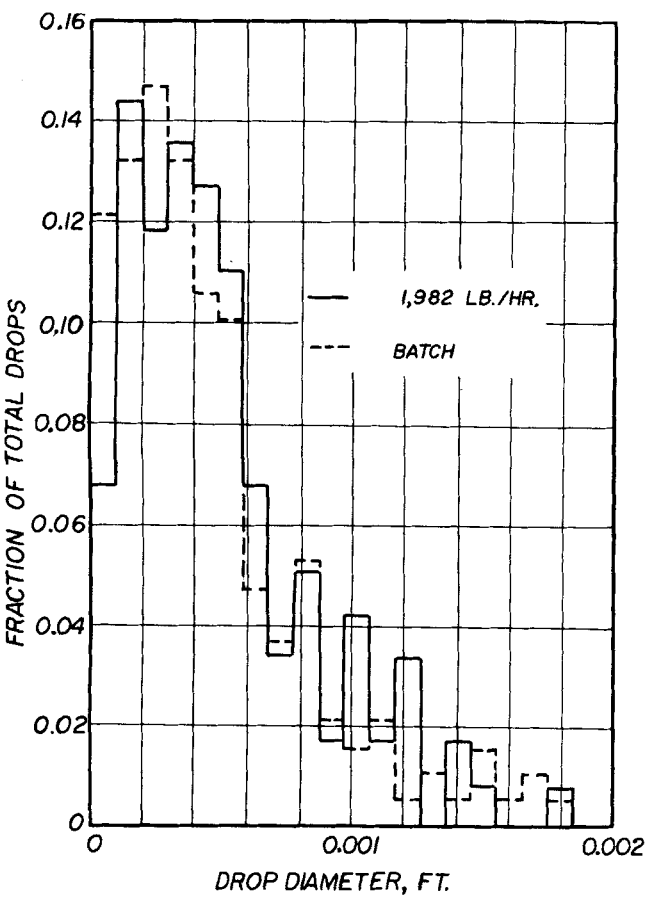

Fig. 4. Drop-size distribution; $\phi_D = 0.0407$, 3 in. impeller, 325 rpm.

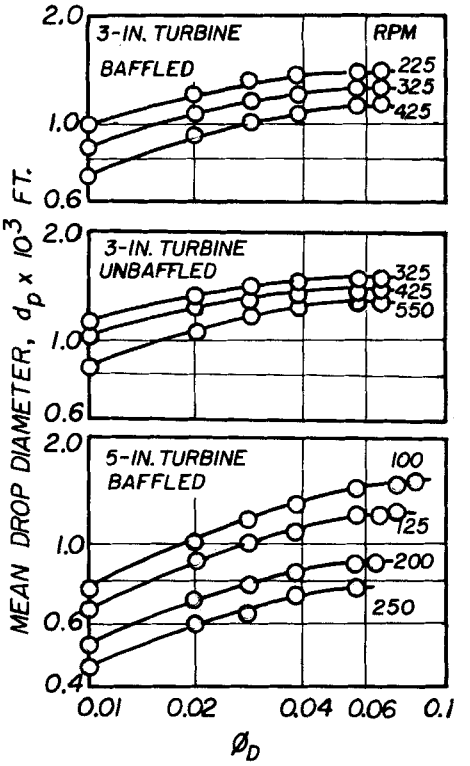

Fig. 5. Mean drop diameter at vessel bottom.

at the same impeller power and ϕ_D, which is in agreement with the findings of Fick (11). The range of power (25 to 300 ft.lb./min.) shown on Figure 3 corresponds to a range 0.25 to 3.0 hp./1,000 gal. vessel volume. The data for the 5 in. impeller are also shown and the small differences indicated are probably related to the change in the ratio, d_t/T. This is true for ϕ_D in the range 0.02 to 0.10.

There is a fifteen to twenty-fold range in the drop size. Figure 4 shows the drop-size distribution as taken from the photographs for the same ϕ_D and impeller speed in both batch and continuous flow runs. The only important difference is in the percentage of small drops, which may be completely dissolved in continuous operation. A t-test of the data for d_p calculated from the photographs showed a 0.95 probability (0.05 level of significance) that d_p's for batch and continuous flow are not significantly different at the same ϕ_D and impeller speed. For continuous flow, a t-test showed a 0.95 probability that d_p's computed from the photographs through Equation (1) and from the light-transmission data and Equation (2) are the same. The conclusions are that specific area at the bottom of the vessel is the same for batch and continuous flow at the same impeller speed and ϕ_D, and that Equation (2) can reasonably be applied elsewhere in the vessel to estimate d_p's.

Most drops are smaller than d_p, although drops smaller than $d_p/2$ contribute very little to specific area and dispersed-phase holdup. Hinze (15) derived an expression for the maximum stable drop size in an isotropically turbulent velocity field. The largest drops observed were consistently 0.5 times this maximum for the baffled vessel (0.4 for the unbaffled vessel), and are probably still smaller near the impeller. Of course, the velocity field in an agitated vessel is highly anisotropic, and in any event the statistical chance of observing the maximum size must be very small. Figure 5 shows that the mean drop size at the bottom appears to be approaching a constant size for ϕ_D greater than 0.05, at least within the range of ϕ_D studied.

SPECIFIC AREA, CONTINUOUS FLOW

Specific area for the vessel as a whole was measured only in conjunction with mass-transfer measurements, and the grouping of the variables is therefore not the best for complete display of the area characteristics. For example, for a constant fraction of liquid to be dispersed in the feed streams, the average fractional dispersed-phase holdup $\phi_{D\,av}$ varies with impeller speed, rising to the fraction in the feed mixture only at high speeds and in the absence of mass transfer. Nevertheless useful conclusions can be drawn.

Figure 6 is typical of how the light-transmission data varied with height in the vessel. The dispersed-phase holdup generally continually rose with height from bottom to top because of the lower density of the dispersed phase. As a result, the specific area is invariably largest in the vicinity of the impeller.

To obtain a true average specific area for the vessel as a whole would require complete exploration of the vessel volume with the light-transmission device. This would be most difficult for a closed vessel operating continuously, therefore the single traverse of the vessel which the light-transmission device provided was taken as the best compromise. The average area computed from this traverse must therefore be recognized as an approximation which may limit the utility of the mass-transfer coefficients computed later. To compute an average, the vessel was divided into three volumes of revolution, of cross section shown in Figure 7, corresponding to the characteristics of curves like that of Figure 6. The mean I_o/I for each zone was computed by graphical integration of the curves like that of Figure 6, and with the measured ϕ_D, Figure 1 and its counterparts for the other two vessel geometries then provided the mean a for each zone. The average a_{av} and holdup $\phi_{D\,av}$ are the volume-weighted averages of a and ϕ_D of the zones, respectively.

Figure 8 typically shows the variation of a_{av} with $\phi_{D\,av}$

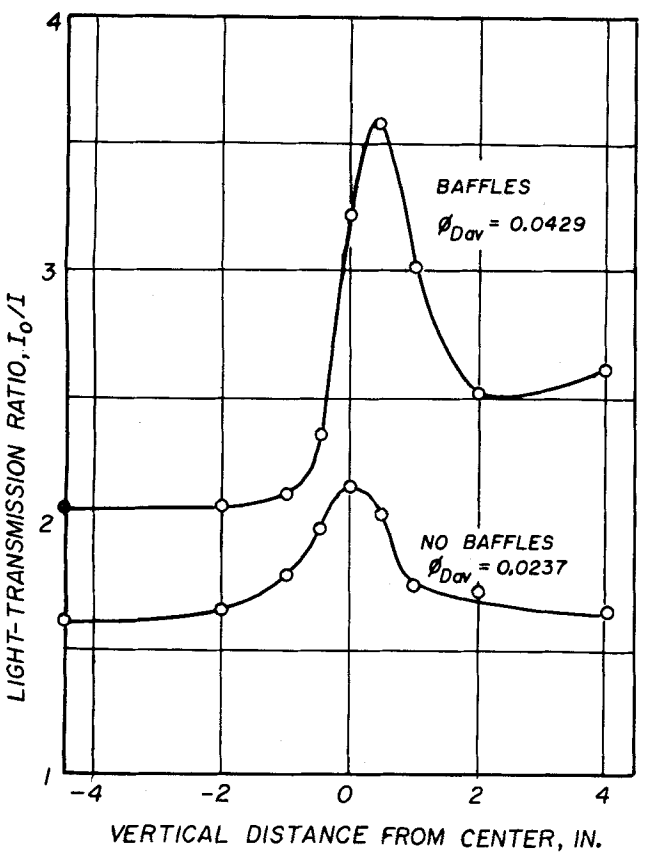

Fig. 6. Typical light-probe traverses; 3 in. impeller, 325 rpm.

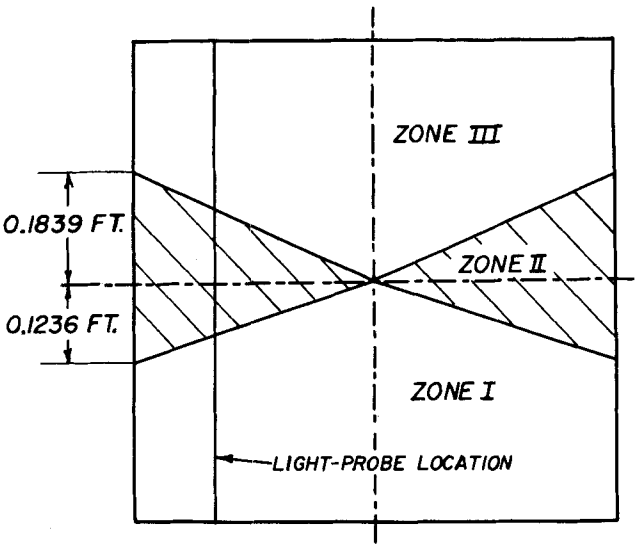

Fig. 7. Zoning of vessel for average area and holdup.

(as produced by different feed ratios) for nearly constant impeller Reynolds Number. There is essentially no effect of flow rate for the baffled vessel over the range studied, but a slight tendency for a_{av} to increase with flow rate was noticed in the absence of baffles. A display of a comparison of observed a_{av} and that computed from the available nonflow correlations for baffled vessels is difficult because both impeller speed and $\phi_{D\,av}$ influence a_{av}, but Figure 9 attempts this to a limited extent. Rodger's correlation (29) is for $\phi_{D\,av} = 0.50$, and is not applicable. The discrepancies between observed and predicted a_{av} by Calderbank (5), Kafarov (20), and Vermeulen (38) are generally large. Possible reasons include (a) the correlations are for the vicinity of the impeller, (b) the interfacial tensions for the correlations are substantially higher, (c) the correlations are for batch operation, and (d) the correlations are for no mass transfer. Thornton's correlations (35), which is for a_{av} and includes ethyl acetate-water, comes close to the data, but the dependency on impeller Reynolds' number is not well handled. His data

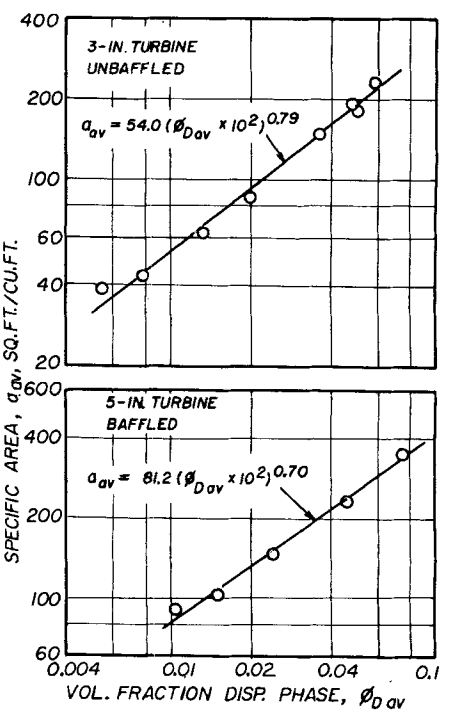

Fig. 8. Mean specific area; flow rate 1,982 lb./hr., N_{Re} = 28,500 to 33,200.

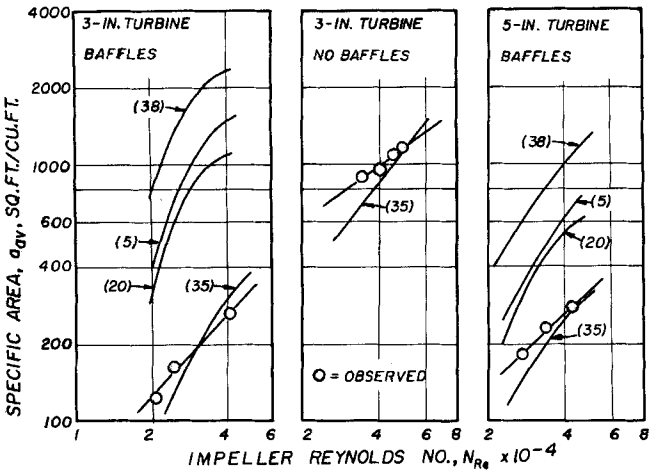

Fig. 9. Comparison of mean specific area with existing correlations; flow rate 1,470 lb./hr., 0.145 lb. organic/lb. water.

do not extend below $\phi_{D\,av}$ below 0.1, however. Because it is based on impeller power rather than on Reynolds' number, it was applied to the data from the unbaffled vessel also, as shown.

MEAN DROP SIZE, CONTINUOUS FLOW

This was computed locally for the three zones of the vessel through Equation (2) from the ϕ_D in the zones and with a obtained from the l_o/l traverse. Because I_o/I is nearly constant in zones I and III, d_p is also (although somewhat larger in the top zone), but it is almost invariably smallest in zone II in the vicinity of the impeller. While not so constant in zones I and II of the unbaffled vessel, nevertheless the regions of essentially constant and of rapidly changing d_p were about the same in volume as in the baffled vessels. Table 1 compares some observed changes in d_p between top and center of the vessel with those computed from Vanderveen's (37). While the magnitude of the difference is about the same, the correlation predicts a decrease in the difference with impeller speed whereas generally an increase was observed. It is known (8, 12, 19) that mass transfer from drops to the continuous phase greatly increases the frequency of coalescence of drops, and since, as will be shown, mass-transfer rates increase with impeller speed, this may be the reason for the observed trend. Vanderveen's observations were made in the absence of mass transfer. Madden (21) observed a rapid increase in coalescence frequency with impeller speed even with mass transfer to the drops.

TABLE 1. DROP SIZE CHANGE IN BAFFLED VESSELS

Impeller speed rpm.	d_p ft. × 10^3, middle	d_p top − d_p middle, ft. × 10^3 obsvd.	Vanderveen (37)
3 in. Turbine, flow rate 1,982 lb./hr.			
205.3	1.187	0.137	0.154
253.5	1.149	0.072	0.138
328.0	0.989	0.186	0.128
435	0.850	0.209	0.118
5 in. Turbine, flow rate = 1,982 lb./hr.			
89.8	1.318	0.005	0.320
111.5	1.110	0.158	0.281
138.7	0.922	0.208	0.262

The average mean drop diameters, $d_{p\,av}$, for the entire vessel were calculated through Equation (2), using a_{av} and $\phi_{D\,av}$. As might be anticipated from the data for a_{av}, they are much larger than those predicted by correlations applicable to the vicinity of the impeller (5, 20, 38), but are reasonably close to those of Thornton (35). They depend less on impeller Reynolds number than was anticipated from the batch correlations, and there is essentially no effect of flow rate in the range studied.

MASS-TRANSFER COEFFICIENTS

For the baffled vessel, the concentrations of ethyl acetate in the bulk continuous liquid x_{A2} were the same at all three levels of sampling; in the unbaffled vessel the difference between x_{A2} at the top and bottom was roughly 2% (in only 3 runs was it greater than 3%), so that both vessels were essentially completely backmixed. The driving force, $x_{A1} - x_{A2}$, was therefore essentially constant throughout the vessel. Three different mass-transfer coefficients are in current use (3, 10), defined for the backmixed vessel by

$$W_A = k_1\, a_{av} V\, (x_{A1} - x_{A2}) \tag{3}$$

$$W_A = k_2\, a_{av} V \ln \frac{W_A/(W_A + W_B) - x_{A2}}{W_A/(W_A + W_B) - x_{A1}} \tag{4}$$

$$W_A - x_{A1}(W_A + W_B) = k_3\, a_{av} V (x_{A1} - x_{A2}) \tag{5}$$

Since both ester and water were extracted, only k_2 and k_3 are really applicable, but in this work the low molar solubility of the ester in water caused the three to differ never by more than 2%, which is within the accuracy of measurement, and they cannot be distinguished. They are reported here as k_C, whose units permit more direct comparison with the work of others:

$$k_1 \doteq k_2 \doteq k_3 = k_C\, (\rho/M)_{av} \tag{6}$$

Typical volumetric coefficients, $k_C\, a_{av}$, as influenced by impeller Reynolds number, are shown in Figure 10 for comparison with other data. The slopes of the lines straddle those of Rushton (31) at $\phi_D = 0.082$ and of Nagata (24) at $\phi_D = 0.0063$, but as shown for the 5 in. turbine there is an important influence of flow ratio. This is emphasized by Figure 1, where ϕ_{Dav} is altered through the feed ratio. The specific areas for the runs of Figure 11, shown in Figure 8, varies less rapidly with ϕ_{Dav} than does $k_C\, a_{av}$, so that ϕ_{Dav} influences k_C as well. This is a phenomenon not observed with suspended solids (2, 7, 13) or dispersed gases (6) and so is peculiar to dispersed liquids.

When k_C is simply plotted against impeller Reynolds number for all the data, a general increase of k_C with N_{Re} for a given vessel geometry is evident, but the scatter due to other influencing variables is relatively great and few conclusions can be drawn. There seems to be little effect of flow rate except in the baffled vessel with

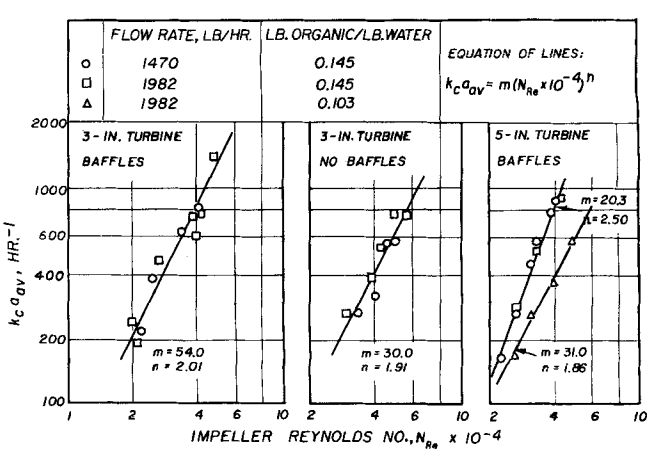

Fig. 10. Volumetric mass-transfer coefficients.

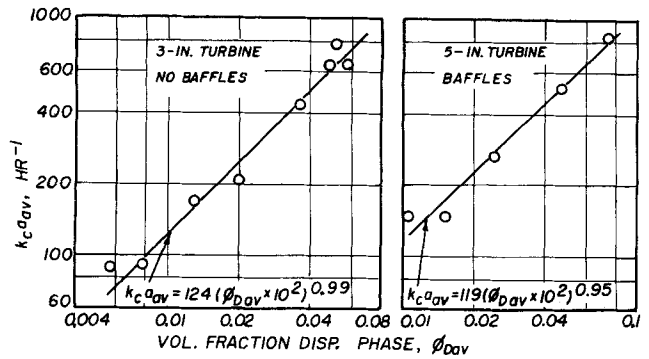

Fig. 11. Influence of dispersed-phase holdup on mass transfer; flow rate 1,982 lb./hr., N_{Re} = 28,500 to 33,200.

the 3 in. impeller (k_C increases slightly with flow rate). Flow ratio, as emphasized by Figures 12 and 13, is evidently a most important variable. Figure 13, where the different ϕ_{Dav} are produced by different flow ratios, might suggest a possible effect of d_p, but Figure 5 shows that d_p becomes almost constant above ϕ_D = 0.05, whereas k_C continues to increase. So again it is holdup which is important.

Before pursuing this further, Figure 14 shows that k_C for the unbaffled vessel is roughly 2.5 times larger than that for the baffled vessel at the same impeller power. Improved stage efficiency in the absence of baffles has been observed before, and it was speculated (25) that this might be due to a reduction of the degree of backmixing in the absence of baffles. But the present study shows that backmixing is essentially complete in both vessels, so that another explanation must be sought.

The observed k_C's are appreciably larger than those given by Barker (2) for relatively large suspended solid particles, who found essentially the same coefficient with and without baffles at the same impeller Reynolds number. They agree moderately well at low impeller Reynolds number in the baffled vessels with the correlation of Harriott (13) for suspended solids, which covers the same range of particle size and impeller power studied here for baffled and unbaffled vessels. But the calculated coefficients become substantially low at increased Reynolds numbers (by factors of 2.2 at N_{Re} = 42,000, for example) and far too low for the unbaffled vessel (by a factor of 4.5 at N_{Re} = 49,000). The same is true for the correlation of Calderbank and Moo-Young (7). None of the correlations anticipate the increase of k_C with increased ϕ_{Dav}.

ROLE OF COALESCENCE

What, then, accounts for the coefficients? It is tentatively suggested that it is the coalescence of droplets as they move radially and vertically away from the impeller to the top and bottom of the vessel, and their redispersion as they circulate back to the impeller along the axis of the vessel. This runs counter to recent theoretical speculations (4) extending conditions found for extraction in a chemically reacting system flowing in a pipe to agitated vessels. But coalescence and redispersion represents the principal immediately demonstrable difference between suspended liquid particles and those for which the correlations were developed. If two drops of ethyl acetate of diameter 0.001 ft. and interfacial tension 6.4 dynes/cm. coalesce, the energy release due to reduction in surface is equivalent to a kinetic energy for the resulting large drop corresponding to a velocity of about 0.8 ft./sec. It is suggested that the violence of the coalescence action may be sufficiently complete to renew the shell of continuous liquid surrounding the drop, thus enhancing the rate of mass transfer.

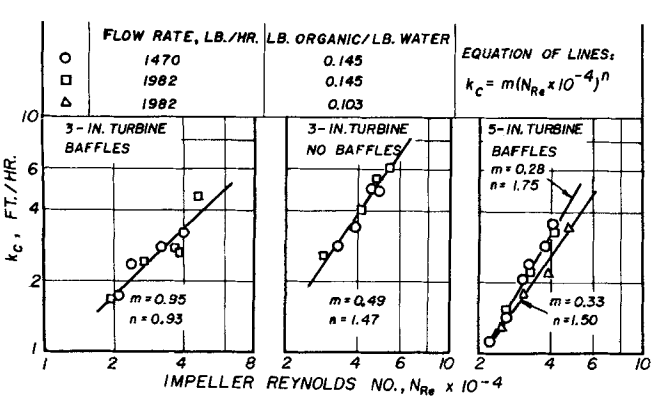

Fig. 12. Continuous-phase mass-transfer coefficients.

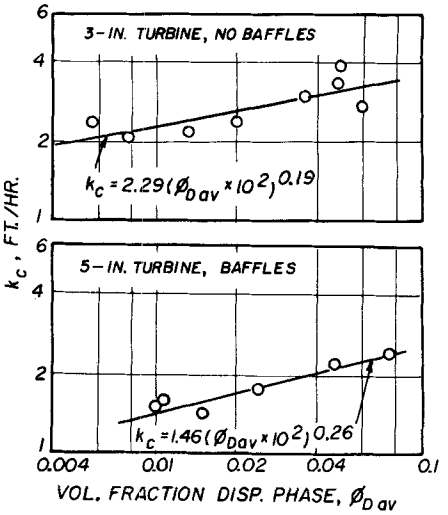

Fig. 13. Influence of dispersed-phase holdup on k_C; flow rate 1,982 lb./hr., N_{Re} = 28,500 to 33,200.

To see what the nature of the effect might be, consider a spherical drop of water-saturated ester of radius r_p, surrounded by a concentric, stagnant, spherical shell of continuous phase, radius R. Immediately after the formation of this drop from a large one, because of the violence of the breakup, the ester concentration in the shell is uniform at c_{A2}. While diffusion of ester into the shell occurs, the concentration remains at c_{A1} at the interface, and at c_{A2} at R. Diffusion occurs for time θ_C, at which time the drop collides with another, coalesces, and is reformed to repeat the process. Fick's second law for diffusive mass transfer,

$$\frac{\partial c_A}{\partial \theta} = D_A \left(\frac{\partial^2 c_A}{\partial r^2} + \frac{2}{r} \frac{\partial c_A}{\partial r} \right) \qquad (7)$$

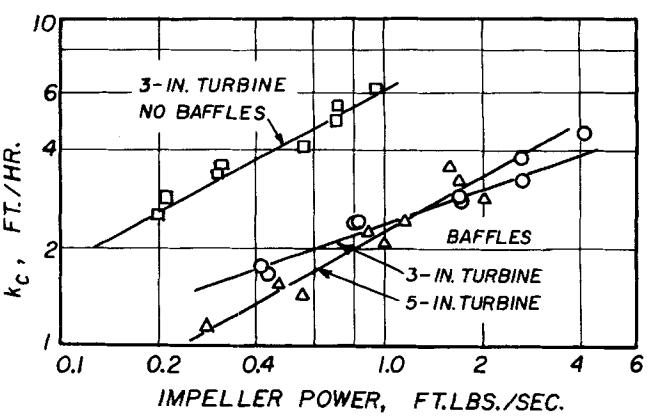

Fig. 14. Influence of baffles and impeller power on k_C; flow rate = 1,470 to 1,982 lb./hr., 0.145 lb. organic/lb. water.

is then to be integrated under the following conditions:

(1) $c_A = c_{A2}$ at $\theta = 0, r_p < r \leq R$

(2) $c_A = c_{A2}$ at $r = R, \theta$

(3) $c_A = c_{A1}$ at $r = r_p, \theta$

It is assumed that the extent of dissolution is small, so that the difficult moving boundary problem (26) need not be considered. The solution to Equation (7) is (33)

$$c_A = \frac{c_{A1} r_p}{r} + \frac{(c_{A2}R - c_{A1} r_p)(r - r_p)}{(R - r_p)r} + \frac{1}{r} \sum_{n=1}^{\infty} \frac{2}{n\pi} (c_{A2} - c_{A1}) r_p \left[\sin n\pi \frac{(r - r_p)}{(R - r_p)} \exp \frac{-n^2\pi^2 D_A \theta}{(R - r_p)^2} \right] \quad (8)$$

An instantaneous mass-transfer coefficient is

$$k'_C = -\left(\frac{D_A}{c_{A1} - c_{A2}} \right) \frac{\partial c_A}{\partial r} \bigg|_{r=r_p} \quad (9)$$

Over the time period θ_C, the time — average k_C is

$$k_C = \frac{\int_0^{\theta_C} k'_C \, d\theta}{\theta_C} \quad (10)$$

These, together with Equation (8), produce

$$k_C = \frac{D_A R}{(R - r_p)r} + \sum_{n=1}^{\infty} \frac{2(R - r_p)}{n^2\pi^2\theta_C} \left[1 - \exp \frac{-n^2\pi^2 D_A \theta_C}{(R - r_p)^2} \right] \quad (11)$$

The first term on the right is a steady state coefficient, the second a transient term.

A typical drop has $r_p = 0.005$ ft., and if it is entitled to an equal share of the entire continuous phase, R is typically 0.015 ft., with $D_A = 3.4(10^{-5})$ sq. ft./hr. For these conditions and θ_C less than 2 sec., the transient term may be taken as 0.9 $(D_A/\theta_C)^{0.5}$, and it contributes 2/3 of the average coefficient at $\theta_C = 2$ sec., as much as 88 % for $\theta_C = 0.2$ sec.

The derivation is unrealistic in that it assumes molecular diffusion, no circulation of the fluid around the drop, no drop oscillation, and no slip or fluctuating velocities. But it leads us logically to write more generally

$$k_C = k_S + \text{const.} \, (D_A/\theta_C)^{0.5} \quad (12)$$

The steady state k_S might be estimated by the best means available, taken tentatively to be the Harriott correlation (13) because it includes particles of the same size range as the present droplets and because it agreed best with the observed mass-transfer coefficients at low impeller Reynolds numbers. Hillestad's work (14) on coalescence rate with systems of high interfacial tensions gives estimates of $1/\theta_C$ which are far lower than those observed from drop-size changes (see below). Howarth's equation (17) estimates rates of collision, not coalescence, and these are extraordinarily high as calculated. It seems best to try to estimate θ_C from the data at hand.

The smallest drops, near the impeller tip, are first thrust radially toward the vessel wall in a region of rapidly diminishing turbulence intensity, zone II. It is assumed that coalescence, but no redispersion occurs here, which is identical with the reasoning of Howarth (18).

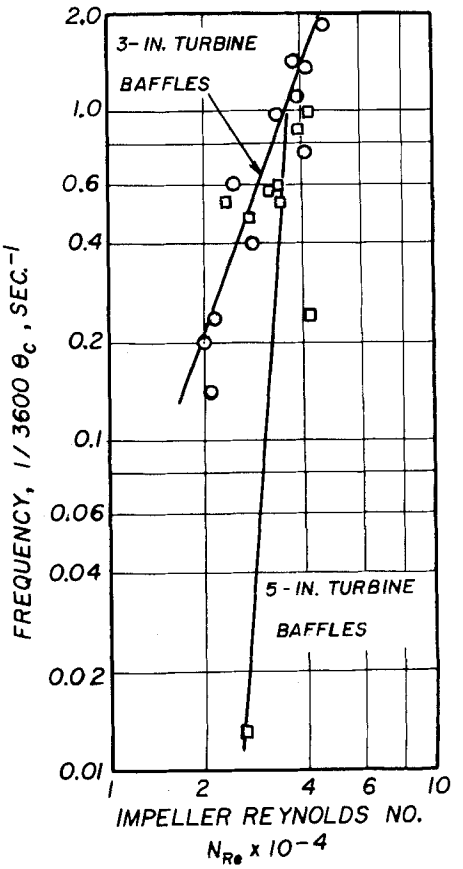

Fig. 15. Coalescence—redispersion frequency; flow rate 1,470 to 1,982 lb./hr., 0.145 lb. organic/lb. water.

During subsequent vertical movement into zones I and III, there are large regions of constant drop size, and it is assumed that neither coalescence nor redispersion occurs. Redispersion is assumed to occur as the liquids move axially toward the center of the impeller in the recirculation path. The number of redispersions equals the number of coalescences per drop, and coalescence frequency per drop equals (no. coalescences/circulation cycle) (circulation frequency). Circulation frequency can be estimated for baffled vessels from Holmes (16).

$$\frac{1}{t_C} = 1.178 \left(\frac{N d_t^2}{T^2} \right) \quad (13)$$

which agrees with the work of Schwartzberg (34). It was verified in the present case by observing the circulation of polyethylene pellets of the same density as ethyl acetate. Unfortunately there is no information on circulation times for unbaffled vessels, and the reasoning from this point on is limited to baffled vessels. θ_C is estimated from the data by

$$\frac{1}{\theta_C} = 2 \left[\frac{(d_{p,T}^3 + d_{p,B}^3)/2 - d_{p,M}^3}{d_{p,M}^3} \right] \frac{1}{t_c} \quad (14)$$

where the coefficient 2 is used to indicate that a redispersion accomplishes the same continuous-phase renewal as a coalescence. This must represent, without question, only the very roughest estimate of the minimum frequency, owing to the assumptions and accumulation of experimental errors, and especially since $d_{p,M}$ is taken at some distance from the impeller tip. The largest source of error is the measured ϕ_D, where a 0.03 ml error in reading volumes of a sample could in some cases result on a

possible 50% error in the difference in d_p for two locations. The errors are aggravated particularly when ϕ_{Dav} is less than 0.03, which invariably results in large increases of ϕ_D from bottom to top of the vessel. Figure 15 indicates the extent of scatter of θ_C for one of the flow ratios. As found by Madden *(21)*, impeller speed and ϕ_{Dav} have a large influence on the frequency.

By using the observed k_C, Harriott's correlation for k_S, and θ_C calculated in the above manner, the average constant of Equation (12) is 3.94, with a standard deviation of 22% for all 38 runs in the baffled vessel with both impellers. If the 7 runs for which θ_C cannot be reasonably estimated are omitted, the average constant becomes 3.83. Typical contributions of the term 3.94 $(D_A/\theta_C)^{0.5}$ to k_C in the expression

$$k_C = k_S + 3.94\,(D_A/\theta_C)^{0.5} \qquad (15)$$

are: zero ($\phi_{Dav} = 0.01$, $N_{Re} = 31{,}000$ and $\phi_{Dav} = 0.0240$, $N_{Re} = 20{,}750$), 17% ($\phi_{Dav} = 0.015$, $N_{Re} = 30{,}000$), 35% ($\phi_{Dav} = 0.0374$, $N_{Re} = 20{,}750$), and 53% ($\phi_{Dav} = 0.0509$, $N_{Re} = 46{,}250$). The unanticipated effect of ϕ_{Dav} on k_C, which increases with increased impeller Reynolds number, seems therefore to be explained. The agreement between k_C observed and calculated from Equation (15) is shown in Figure 16 for the 31 runs. Admittedly the scatter is considerable, due largely to the frequency data. But it is felt that the relationship is sufficiently well established to warrant further consideration of the coalescence phenomenon as a strong influence on the mass-transfer coefficients.

In the unbaffled vessel, it has been shown that k_C is itself appreciably larger, and that lack of backmixing is not an important consideration. Use of Harriott's correlation for k_S for unbaffled vessels would require even a larger contribution of coalescence toward k_C than for baffled vessels, since his correlation relies heavily on impeller power. If it is assumed that the drops at the impeller tip are of about the same size for baffled and unbaffled vessels, then the larger average $d_{p\,av}$ observed here in the absence of baffles would seem to confirm the greater importance of coalescence in this case, at least qualitatively. These matters are being pursued further.

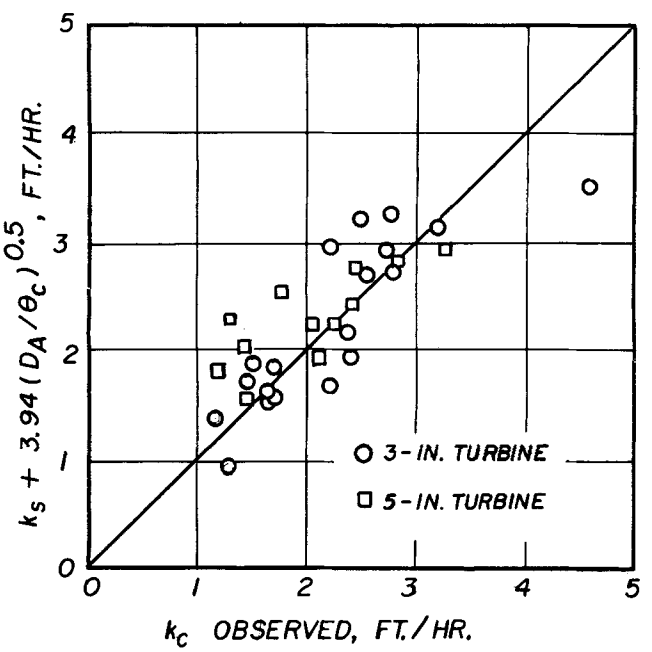

Fig. 16. Comparison of k_C with Equation (15).

ACKNOWLEDGMENT

This work was done under Grant G-21526 of the National Science Foundation, whose support is most gratefully acknowledged. Herbert Setzer built the equipment used.

NOTATION

a = local mean specific interfacial area, sq. ft./cu. ft.
a_{av} = mean specific interfacial area, average for the vessel, sq. ft./cu. ft.
c = concentration, lb. moles/cu. ft.
d_i = individual drop diameter, ft.
d_p = local mean drop diameter, ft.
$d_{p\,av}$ = mean drop diameter, average for the vessel, ft.
d_t = turbine diameter, ft.
D = diffusivity, sq. ft./hr.
I_o/I = incident light intensity/emergent light intensity
k_C = average continuous-phase mass-transfer coefficient, lb. moles/hr. (sq. ft.) (lb. moles/cu. ft.)
k'_C = instantaneous continuous-phase mass-transfer coefficient, lb. moles/hr. (sq. ft.) (lb. moles/cu. ft.)
k_D = dispersed-phase mass-transfer coefficient, lb. moles/hr. (sq. ft.) (lb. moles/cu. ft.)
k_S = steady-state continuous-phase mass-transfer coefficient, lb. moles/hr. (sq. ft.) (lb. moles/cu. ft.)
k_1,k_2,k_3 = continuous-phase mass-transfer coefficients, lb. moles/hr. (sq. ft.) (mole fraction)
K = overall mass-transfer coefficient, lb. moles/hr. (sq. ft.) (lb. moles/cu. ft.)
M = molecular weight, lb./lb. mole
n = a number
N = frequency of revolution, rev./hr.
N_{Re} = impeller Reynolds number, dimensionless
r = radius, ft.
r_p = mean drop radius, ft.
R = radius of continuous-phase shell, ft.
t_C = circulation time, hrs.
T = vessel diameter, ft.
V = vessel volume, cu. ft.
W = extraction rate, lb. moles/hr.
x = concentration, mole fraction

Greek Letters

θ = time, hrs.
θ_C = time between coalescences, hr.
ϕ_D = local volume fraction dispersed phase
ϕ_{Dav} = volume fraction dispersed phase, average for the vessel
ρ = density, lb./cu. ft.

Subscripts

A = ethyl acetate
B = water; bottom of the vessel
M = middle of the vessel
T = top of the vessel
1 = in the continuous phase at the interface
2 = in the bulk continuous phase

LITERATURE CITED

1. Akell, R. B., *Chem. Eng. Progr.*, **62**, No. 9, 50 (1966).
2. Barker, J. J., and R. E. Treybal, *AIChE J.*, *6*, 289 (1960).
3. Bird, R. B., W. E. Stewart, and E. N. Lightfoot, "Transport Phenomena," John Wiley, New York (1960).
4. Boyadzhiev, L., and D. Elenkov, *Chem. Eng. Sci.*, **21**, 955 (1966).
5. Calderbank, P. H., *Trans. Inst. Chem. Engrs. (London)* **36**, 443 (1958).
6. *Ibid.*, 37, 173 (1959).
7. ———, and M. B. Moo-Young, *Chem. Eng. Sci.* **16**, 39 (1961).

8. Charles, G. E., and S. G. Mason, *Colloid Sci.*, **15**, 236 (1960).
9. Colburn, A. P., and D. G. Welsh, *Trans. Am. Inst. Chem. Engrs.* **38**, 179, (1942).
10. Drew, T. B., and A. P. Colburn, *ibid.* **33**, 197 (1937).
11. Fick, J. L., H. E. Rea, and T. Vermeulen, *U.S. Atomic Energy Comm.* **UCRL-2545** (1954).
12. Groothius, H., and F. J. Zuiderweg, *Chem. Eng. Sci.*, **12**, 288 (1960); **19**, 63 (1964).
13. Harriott, P., *AIChE J.*, **8**, 93 (1962).
14. Hillestad, J. G., and J. H. Rushton, paper presented at AIChE Meeting, Columbus, Ohio (May, 1966).
15. Hinze, J.O., *AIChE J.*, **1**, 289 (1955).
16. Holmes, D. B., R. M. Voncken, and J. A. Dekker, *Chem. Eng. Sci.*, **19**, 201 (1964).
17. Howarth, W. J., *ibid.*, **19**, 33 (1964).
18. ———, *AIChEJ.*, **13**, 1007 (1967).
19. Johnson, S. F., and H. Bliss, *Trans. Am. Inst. Chem. Engrs.*, **42**, 331 (1946).
20. Kafarov, V. V., and B. M. Babanov, *Zhur. Priklad. Khim.*, **32**, 789 (1959).
21. Madden, A. J., and G. L. Damerell, *AIChE J.*, **8**, 233 (1962).
22. Middleman, S., *ibid.*, **11**, 750 (1965).
23. Miller, D. N., *Ind. Eng. Chem.*, **56**, No. 10, 18 (1964).
24. Nagata, S., and I. Yamaguchi, *Mem. Fac. Eng. Kyoto Univ.*, **22**, 249 (1960).
25. Overcashier, R. H., H. A. Kingsley, and R. B. Olney, *AIChE J.*, **2**, 529 (1956).
26. Ready, D. W., and A. R. Cooper, *Chem. Eng. Sci.*, **21**, 917 (1966).
27. Reman, F. H., *Chem. Eng. Progr.*, **62**, No. 9, 56 (1966).
28. Rodger, W. A., *U.S. Atomic Energy Comm.*, **ANL-5575** (1956).
29. ———, and V. G. Trice, *ibid*, **ANL-5512** (1956).
30. ———, V. G. Trice, and J. H. Rushton, *Chem. Eng. Progr.*, **52**, 515 (1956).
31. Rushton, J. H., S. Nagata, and T. B. Rooney, *AIChE J.*, **10**, 298 (1964).
32. ———, and J. Y. Oldshue, *Chem. Eng. Progr.*, **49**, 161 (1953).
33. Schindler, H. D., Ph.D. thesis, New York Univ., New York (1967).
34. Schwartzberg, H. G., and R. E. Treybal, *Ind. Eng. Chem. Fundamentals*, **7**, 1, 6 (1968).
35. Thornton, J. D., and B. A. Bouyatiotis, *Ind. Chemist*, **39**, 298 (1963).
36. Treybal, R. E., "Liquid Extraction," 2nd ed., McGraw-Hill, New York (1963).
37. Vanderveen, J. H., *U.S. Atomic Energy Comm.*, **UCRL-8733** (1960).
38. Vermeulen, T., G. M. Williams, and G. E. Langlois, *Chem. Eng. Progr.*, **51**, 85F (1955).

Manuscript received September 11, 1967; revision received December 18, 1967; paper accepted January 10, 1967. Paper presented at AIChE Tampa meeting.

Nonuniform Initiation of Photoreactions. III. Reactant Diffusion in Single-Step Reactions

F. B. HILL and N. REISS
Brookhaven National Laboratory, Upton, New York

L. H. SHENDALMAN
Yale University, New Haven, Connecticut

The influence of nonuniform initiation on conversion in single-step photoreactions is examined theoretically. Reaction types studied include reaction following absorption by reactant and photosensitized reaction. The batch slab reactor and the laminar flow tubular reactor with outside radiation are considered. In the case of reaction following absorption by reactant in the batch slab reactor, nonuniform initiation is found to have no influence on conversion, whereas for the other combinations of reaction and reactor its presence requires the specification of diffusion as well as kinetic parameters in order to characterize the conversion history unequivocally. The characteristics of conversion histories in the presence of nonuniform initiation are determined, and the influence of nonuniform initiation on chemical measurements of radiation and on tubular reactor performance in the neighborhood of laminar-turbulent flow transitions is discussed.

The complete determination of the kinetic behavior of isothermal photoreactions in the presence of strong absorption of radiation often requires a knowledge not only of chemical rates but also of rates of diffusion or mixing in the directions of radiation attenuation. The response to the nonuniform initiation resulting from strong absorption depends on the reaction mechanism and on the relative rates of mass transfer, reaction, and radiation absorption. When reactive intermediates disappear in pairs, the observed reaction rate will vary with the extent of movement of intermediates. When intermediates singly disappear, movement of intermediates has no effect on reaction rate. The influence of nonuniform initiation on photoreactions in which movement of reactive centers is important has been discussed in earlier papers in this series (*1, 2*).

N. Reiss is at Columbia University, New York, New York.

In the present paper, reactions are considered in which the extent of movement of intermediates is unimportant, and attention is centered on the effect of reactant movement. We deal with reactions which may be represented by the single step,

$$A \xrightarrow{h\nu} B$$

While this reaction may actually proceed via a complex sequence of elementary reactions of reactants and intermediates, the kinetic features of present interest are nevertheless embodied in the single step shown. At the same time, examination of the influence of nonuniform initiation on this reaction may be helpful in understanding effects in complex mechanisms, since the reaction is of the nature of a reaction initiation step. Also, the results of the present analysis may be of use in assessing the importance of diffusion and mixing on chemical mea-